Substituent Effects and Charge Delocalization Mode in Chrysenium, Benzo[*c*]phenanthrenium, and Benzo[*g*]chrysenium Cations: A Stable Ion and Electrophilic Substitution Study

Kenneth K. Laali* and Takao Okazaki

Department of Chemistry, Kent State University, Kent, Ohio 44242

Subodh Kumar

Environmental Toxicology & Chemistry, Great Lakes Center for Environmental Research and Education, State University of New York College at Buffalo, 1300 Elmwood Avenue, Buffalo, New York 14222

Sergio E. Galembeck

LAMMOL, Departamento de Quimica, FFCLRP-USP, SP-Brazil

klaali@kent.edu

Received August 21, 2000

The first series of persistent carbocations derived from mono- and disubstituted chrysenes Ch (5-methyl- **3**, 2-methoxy- **19**, 2-methoxy-11-methyl- **20**, 2-methoxy-5-methyl- **21**, and 9-methyl-4*H*-cyclopenta[*def*]chrysene **22**), monosubstituted benzo[*c*]phenanthrenes BcPh (3-methoxy- **23**, 3-hydroxy- **24**), and monosubstituted benzo[*g*]chrysenes BgCh (12-methoxy- **25**; 12-hydroxy- **26**) were generated in FSO_3H/SO_2ClF or FSO_3H-SbF_5 (4:1)/SO_2ClF and studied by low-temperature NMR at 500 MHz. The methoxy and methyl substituents direct the protonation to their respective *ortho* positions. Whereas parent Ch **1** is protonated at C-6/C-12, **3** is protonated at C-6 (**3aH**$^+$) and at C-12 (**3bH**$^+$) with the latter being the thermodynamic cation. The 2-methoxy-Ch **19** is protonated at C-1 to give two conformationally distinct carboxonium ions (**19aH**$^+$**/19bH**$^+$). In the disubstituted Ch derivatives **20** and **21**, the 2-methoxy overrides the 5-methyl and the predominant carbocations formed are via attack *ortho* to methoxy. For the methano derivative **22** (Me at C-9), a 3:1 mixture of **22aH**$^+$**/22bH**$^+$ is formed. For parent BcPh **13**, nitration and benzoylation are directed to C-5. With 3-methoxy-BcPh **23**, the site of attack moves to C-4, thus producing two conformationally distinct carboxonium ions (**23aH**$^+$**/23bH**$^+$), whereas conventional nitration gave a 2:1 mixture of **23aNO$_2$** and **23bNO$_2$**. In 3-hydroxy-BcPh **24**, the carboxonium ion **24H**$^+$ is exclusively formed. For parent BgCh **16**, protonation, nitration, and benzoylation are all directed to C-10 (**16H**$^+$, **16NO$_2$**, **16COPh**), but presence of OMe or OH substituent at C-12 changes the site of attack to C-11. Charge delocalization mode is probed based on magnitude of $\Delta\delta$ ^{13}Cs and conformational aspects via NOED experiments. Complete NMR data are also reported for several benzoylation/nitration products. Using ab initio/GIAO (and NICS), the NMR chemical shifts (and aromaticity) in model carbocations **A**−**D** were evaluated. This work represents the first direct study of the carbocations derived from the methyl-, methoxy-/hydroxy-derivatives of three important classes of bay-region and fjord-region PAHs whose diol-epoxides extensively bind to DNA. It also extends the available data on electrophilic chemistry of BcPh and BgCh.

Introduction

In PAHs, the "correct" substitution has a major impact on biological activity. The concept has been well tested over the years in several classes of planar and nonplanar PAHs for which the diol-epoxide activation path is metabolically significant.[1−3] In general, introduction of methyl (or other small electron-releasing groups) at sterically crowded regions increases mutagenic/tumorigenic potency in the PAHs, and their epoxide and diol-epoxides exhibit greatly enhanced DNA binding ability. These effects become more pronounced in nonplanar PAHs which possess fjord region(s).[4−7] Increased biological activity in strained PAH-epoxides and diol-epoxides may be related to increased epoxide reactivity and relief of steric strain as a driving force for the formation of bay-region and fjord-region carbocations. It is also suggested that steric factors could slow enzymatic detoxification (epoxide to diol), thus increasing the lifetime of the epoxide and hence the likelihood of attack by DNA.[8]

* Corresponding author: Tel: 330-672-2988. Fax: 330-672-3816.

(1) Harvey, R. G. *Polycyclic Aromatic Hydrocarbons*; Cambridge Monographs on Research, Cambridge University Press: Cambridge, UK, 1991; Chapt. 3.

(2) Hecht, S. S.; Amin, S.; Melikian, A. A.; LaVoie, E. J.; Hoffmann, D. In *Polycyclic Hydrocarbons and Carcinogenesis*; Harvey, R. G., Ed.; ACS Symposium Series 283, American Chemical Society: Washington, DC, 1985; Chapter 5.

(3) Coombs, M. M.; Bhatt, T. S. *Cyclopenta[a]phenanthrene*; Cambridge University Press: Cambridge, UK, 1987; Chapter 6.

(4) Chang, H.-F.; Cho, B. P. *J. Org. Chem.* **1999**, *64*, 9051.

(5) Kiselyov, A. S.; Lee, H.; Harvey, R. G. *J. Org. Chem.* **1995**, *60*, 6123.

(6) Bushman, D. R.; Grossman, S. J.; Jerina, D. M.; Lehr, R. E. *J. Org. Chem.* **1989**, *54*, 3533.

(7) Agrawal, S. K.; Sayer, J. M.; Yeh, H. J. C.; Pannell, L. K.; Hilton, B. D.; Pigott, M. A.; Dipple, A.; Yagi, H.; Jerina, D. M. *J. Am. Chem. Soc.* **1987**, *109*, 2497.

10.1021/jo001268b CCC: $20.00
Published on Web 01/16/2001

Scheme 1

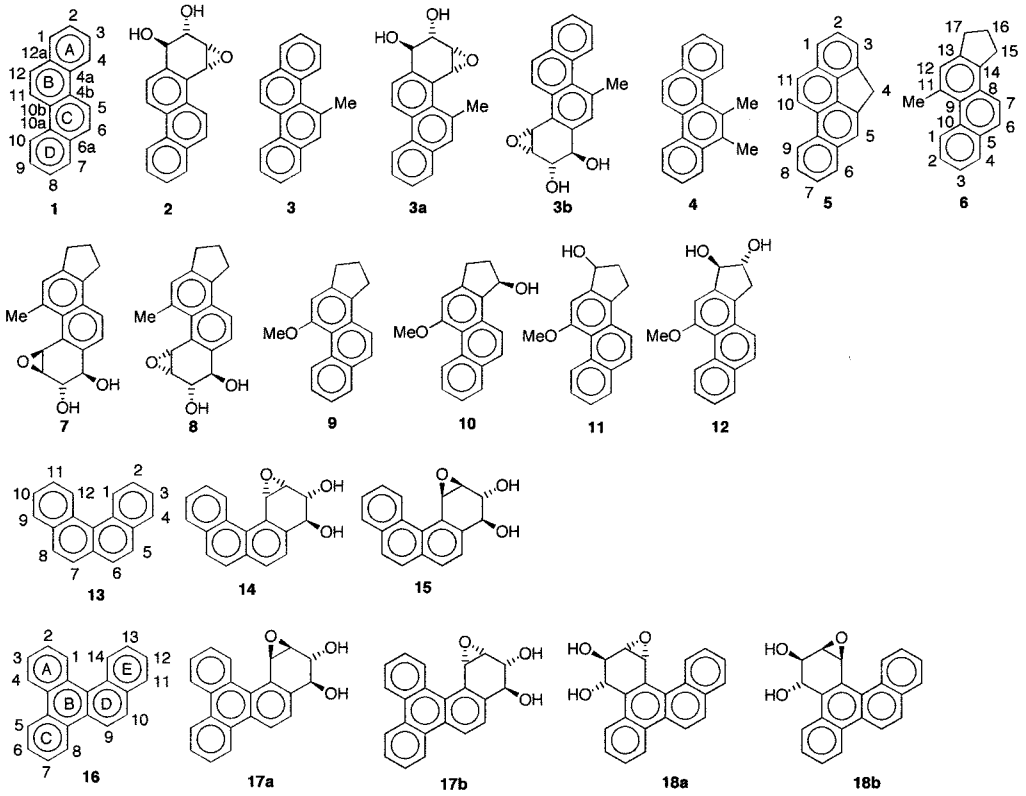

In chrysene Ch **1** (inactive as a complete carcinogen/weak tumorigen), the principle active metabolite is **2** (see Scheme 1). Introduction of methyl group at C-5 makes a potent carcinogen (**3**) equal to benz[*a*]pyrene BaP, whose major active metabolite is **3a**. Although the D-ring is also metabolized (**3b**), it is biologically less important.[1,9a] The nonplanar 5,6-dimethyl derivative (**4**) is also a potent carcinogen.[9b] Introduction of a methano bridge (**5**) increases electrophilic reactivity even though one bay region is removed. Here, apart from the diol-epoxide activation route an additional reactive site for DNA binding to **5** is created via hydroxylation−esterification at the bridge leading to the carbocation.[9c]

In cyclopenta[*a*]phenanthrene C_p[*a*]P, activity enhancement is induced when Me or OMe group is introduced into the bay-region at C-11 (**6** and **9**).[3,10,11] For **6**, the principle diol-epoxides are **7** and **8**, whereas for the unusually reactive **9** the 15-ol **10**, 17-ol **11**, and 16,17-diol **12** are produced and **11** is believed to be the proximate carcinogen.[11] Additional increase in steric crowding at C-11 (Et, i*Pr*, n-Bu) reduces carcinogenicity because the approach of target DNA nucleotide is now prevented.[12] The same reasoning could be applicable to BaP for which methyl introduction in the annelated ring reduces carcinogenicity.[1]

BcPh **13** (weakly carcinogenic but highly mutagenic) has a fjord region and a twisted framework (31° of the plane).[13,14] Its diol epoxides **14** and **15** form covalent adducts via the benzylic carbon to the exocyclic amino group of dG and dA.[4,7] Methyl introduction at C-2 abolishes the activity, whereas the 3-, 4-, 5-, and 6-Me derivatives are active.[1] Nitration, bromination, and acetylation of BcPh have been reported, with preferential substitution occurring at C-5.[15] All possible monofluoro derivatives of **13** have been synthesized.[16] Interestingly, fluorine substitution at C-6 (K-region) increased carcinogenicity over 4-fold. BgCh **16** is a potent carcinogen whose fjord-region diol epoxides (**17**, **18**) have been synthesized.[5,6,17] Among them the 11,12-diol-13,14-epoxides (**17a**, **17b**) are the ultimate carcinogens.[6] Acetylation and trifluoroacetylation of BgCh resulted in substitution mainly at C-10.[18] In relation to our previous and ongoing direct studies of PAH carbocations as models of PAH electrophiles,[19] and α-PAH-substituted carbocations as epoxide ring opening models,[20] the present study

(8) See ref 5 and pertinent references therein.

(9) (a) Harvey, R. G. In *Polycyclic Hydrocarbons and Carcinogenesis*; Harvey, R. G., Ed.; ACS Symposium Series 283, American Chemical Society: Washington, DC, 1985; Chapter 3. (b) Szeliga, J.; Amin, S.; Zhang, F.-J.; Harvey, R. G. *Chem. Res. Toxicol.* **1999**, *12*, 347. (c) Dai, W.; Abu-Shqara, E.; Harvey, R. G. *J. Org. Chem.* **1995**, *60*, 4905.

(10) Bhatt, T. S.; Coombs, M. *Polycyclic Aromat. Compd.* **1990**, *1*, 55.

(11) Catterall, F. S.; Coombs, M. M.; Ioannides, C.; Walton, K. *Mutat. Res.* **2000**, *465*, 85.

(12) Bhatt, T. S.; Hadfield, S. T.; Coombs, M. M. *Carcinogenesis* **1982**, *3*, 667.

(13) Harvey, R. G. *Polycyclic Aromatic Hydrocarbons*; Wiley/VCH: New York, 1997; Chapt. 2.

(14) Herndon W. C. In *Polynuclear Aromatic Hydrocarbons*; Ebert, L. E., Ed.; Advances in Chemistry Series 217, American Chemical Society: Washington, DC, 1988.

(15) (a) Newman, M. S.; Kosak, A. I. *J. Org. Chem.* **1949**, *14*, 375. (b) Sarobe, M.; Jenneskens, L. W.; Wesseling, J.; Wiersum, U. E. *J. Chem. Soc., Perkin Trans. 2* **1997**, 703.

(16) Mirsadeghi, S.; Prasad, G. K. B.; Whittakar, N.; Thakker, D. R. *J. Org. Chem.* **1989**, *54*, 3091.

(17) Utermoehlen, C. M.; Singh, M.; Lehr, R. E. *J. Org. Chem.* **1987**, *52*, 5574.

(18) Kiselyov, A. S.; Harvey, R. *Tetrahedron Lett.* **1995**, *36*, 4005.

(19) (a) Laali, K. K.; Hollenstein, S.; Galembeck, S. E.; Coombs, M. M. *J. Chem. Soc., Perkin Trans. 2* **2000**, 211. (b) Laali, K. K.; Tanaka, M. *J. Org. Chem.* **1998**, *63*, 7280. (c) Laali, K. K.; Hollenstein, S.; Hansen, P. E. *J. Chem. Soc., Perkin Trans. 2* **1997**, 2207. (d) Laali, K. K.; Hollenstein, S.; Harvey, R. G.; Hansen, P. E. *J. Org. Chem.* **1997**, *62*, 4023. (e) Laali, K. K.; Okazaki, T.; Coombs, M. M. *J. Org. Chem.* **2000**, *65*, 7399.

(20) (a) Laali, K. K.; Hollenstein, S. *J. Chem. Soc., Perkin Trans. 2* **1998**, 897. (b) Laali, K. K.; Hansen, P. E. *J. Org. Chem.* **1997**, *62*, 5804. (c) Laali, K. K.; Tanaka, M.; Hollenstein. S.; Cheng, M. *J. Org. Chem.* **1997**, *62*, 7752.

focuses on three important classes of alternant PAHs Ch **1**, BcPh **13**, and BgCh **16** and some of their *key* substituted derivatives. The highlights of this investigation are to ascertain the influence of Me, OMe, and OH substituents in directing the site of attack and the mode of charge delocalization (and conformational aspects) in the resulting carbocations and carboxonium ions. Using nitration and benzoylation as model reactions, several derivatives were synthesized and their NMR spectra were fully assigned. Charge delocalization and aromaticity in model carbocations derived from the biologically important epoxides of BgCh, BcPh, and Ch were evaluated using ab initio/GIAO and NICS methods. Protonation of the fjord-region ketone **27** is also reported.

Results and Discussion

Background to the Present Investigation. Access to the strategically substituted methyl-, methoxy- (and hydroxy-) derivatives of Ch, BcPh, and BgCh as well as to parent BcPh and BgCh became possible via an efficient route developed by Kumar[21] which uses a Suzuki cross-coupling reaction as a key step.

In a previous stable ion study,[19d] we showed that parent **1** and its 6-halo derivatives are protonated at C-12 and 4*H*-cyclopenta[*def*]chrysene at C-5 (*peri* to methano bridge). Chrysenium cations with a methyl and methoxy substituent were hitherto unknown. Carbocations derived from **3**, **19**, **20**, **21**, and **22** are generated and examined in the present work to elucidate substituent effects and the charge delocalization mode for comparison with the analogues examined earlier. Carbocations derived from the nonplanar, fjord-region PAHs represented a virgin territory for charge delocalization mapping and substituent effect study. Conventional electrophilic substitution work had pointed to C-5 in BcPh (bromination, nitration, acetylation) and C-10 in BgCh (acetylation, trifluroacetylation), but their substituted derivatives had not been studied.

NMR Assignments (Figure S1 and Figure S2 in Supporting Information). Detailed NMR assignments for the precursors, carbocations and the substitution products were based on ^{1}H, ^{13}C, H/H COSY, C/H HETCOR (or HMQC), COLOC (or HMBC), and NOED spectra.

NMR Features in the Neutrals. Irradiation of OMe protons in the neutral PAHs gave concurrent NOE enhancements for H-1/H-3 (*ortho*) in **19** and **20**, for H-2/H-4 in **23**, and for H-11/H-13 in **25**. However, these NOE enhancements were larger for H-1 (**19** and **20**), H-4 (**23**), and H-11 (**25**). In **3** and **21**, NOE enhancement was observed between the methyl and H-4 (*peri*)/H-6 (*ortho*); furthermore, methyl introduction deshields the H-4 and shields the H-6. In the fjord-region PAHs (**13**, **16**), methoxy substitution shields both H-2/H-4 in **13** and H-11/H-13 in **16** (an OH group has the same effect). The BcPh and BgCh and their substituted derivatives have very diagnostic highly deshielded fjord-region protons. NMR assignments for parent Ch, BcPh, and BgCh had been reported by Bax et al.[22a] and by Hoffman et al.[22b] using 2D-techniques. These are in very close agreement with ours. In the fjord-region ketone, the CO group has a strong shielding effect on H-14. Whereas this feature was previously noted,[23] the previous assignments of H-14 and H-8 should be reversed. NOE effects were observed between H-14 and CO−CH_2 and H-8/H-9 across the fjords and bay-region NOE effects were detected between H-10/H-11 and H-5/CH_2.

Scheme 2

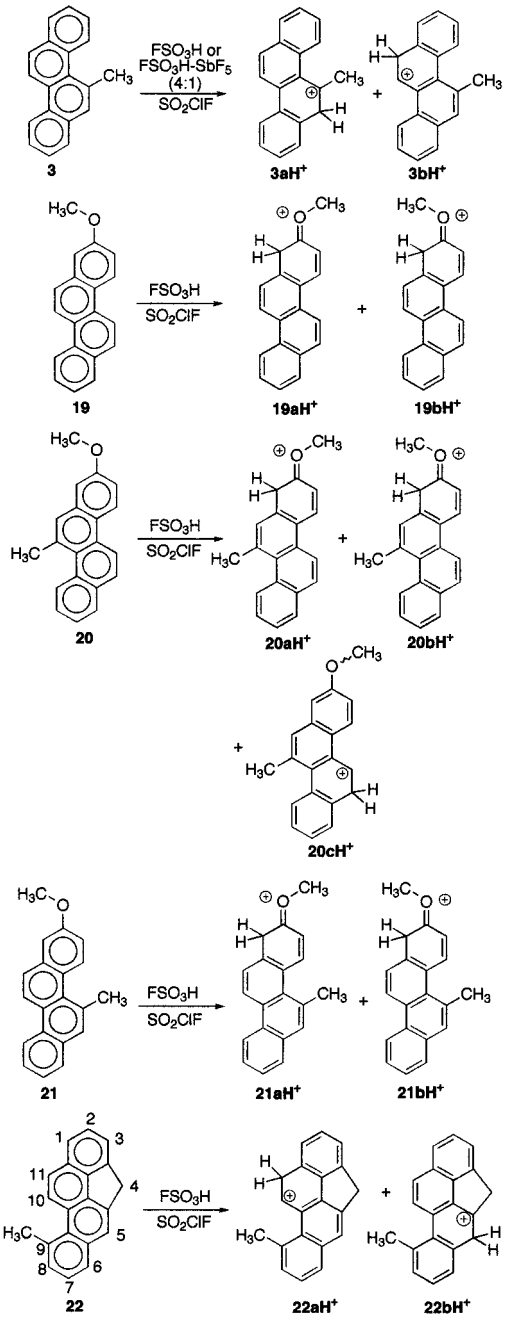

Monoprotonation of Substituted Chrysenes (Scheme 2 and Figure S1)

(a) 5-Methylchrysene (3). Low-temperature reaction of **3** with FSO_3H-SbF_5 (4:1)/SO_2ClF gave a mixture of two chrysenium cations **3aH**$^+$ and **3bH**$^+$ (dark-red) with protonation taking place at C-6/C-12 (3:1 ratio at −70 °C). Upon warming the superacid solution (−70 °C to −30

(21) (a) Kumar, S. *J. Org. Chem.* **1997**, *62*, 8535. (b) Kumar, S. *Tetrahedron Lett.* **1996**, *37*, 6271. (c) Kumar, S. *J. Chem. Soc., Perkin. Trans. 1* **1988**, 3157.

(22) (a) Bax, A.; Ferretti, J. A.; Nashed, N.; Jerina, D. M. *J. Org. Chem.* **1985**, *50*, 3029. (b) Hoffman, R. E.; Weitz, A.; Rabinovitz, M. *J. Magn. Reson, Ser. A* **1993**, *102*, 1.

(23) Lakshman, M. K.; Lehr, R. E. *Synth.Commun.* **1994**, *24*, 2973.

°C), **3aH**$^+$ completely isomerized to **3bH**$^+$, indicating that the former is the kinetic carbocation and the latter the thermodynamic cation. AM1 predicts that among all possible arenium ions to be formed **3aH**$^+$/**3bH**$^+$ are in fact the most favored, with **3bH**$^+$ computed to be 3 kcal/mol higher in energy. In the minimized structures, both arenium ions are twisted owing to the methyl group at C-5. Protonation of **3** with FSO_3H/SO_2ClF yielded only **3aH**$^+$ (dark-red solution at dry ice−acetone temperature). When the solution was warmed (−70 °C to −30 °C), **3aH**$^+$ isomerized to produce a mixture of carbocations and shortly thereafter decomposition set in (concomitant line broadening in the NMR spectra). Therefore, in this case, higher regioselectivity was achieved in the higher acidity superacid solvent.

In **3aH**$^+$, the bay-region protons H-10/H-11/H-4 are noticeably shielded relative to **3**. NOE effects were observed between the Me and H-6(CH_2)/H-4, between H-6/H-7, between H-10/H-11, and between H-1/H-12. The most deshielded carbon resonance in **3aH**$^+$ is C-5 (δ 198.4). Positive charge resides predominantly at C-5/C-10b/C-12 and to a lesser extent at C-6a/C-8. Because several other carbons are also positive a clear charge alternation path is not established. The proton resonances in FSO_3H-SbF_5 (4:1)/SO_2ClF solvent were more deshielded than those in FSO_3H/SO_2ClF medium. This is probably a combination of more complete protonation and less nucleophilic/bulkier counterion in the former system. For **3bH**$^+$ the H-4/H-10 are shielded and H-11 is most deshielded (δ 10.15). There is NOE between the methyl and H-6/H-4; H-6/H-7; H-10/H-11, and between H-1/H-12. The most deshielded ^{13}C resonances are *the ortho/para* (C-11, C-4b, C-12a) and the C-5. Since C-2/C-9/C-10 are also positive, no regular charge alternation path is established.

(b) 2-Methoxychrysene (19). Introduction of OMe group at C-2 directs the substitution to C-1. Thus low-temperature reaction of **19** with FSO_3H/SO_2ClF gave a dark-red solution (initially a red precipitate was also observed which subsequently dissolved), whose NMR spectra are consistent with protonation at C-1 resulting in two conformationally distinct carboxonium ions **19aH**$^+$/**19bH**$^+$ (3:2 ratio at −50 °C). Specific conformations could not be decided based on NOE experiments since irradiation of the methyls (δ 4.50, 4.38) gave NOE enhancement for both H-1 (CH_2; δ 3.81/3.59) and H-3 (δ 7.02/7.13). In concert with experiment, AM1 predicted that among all possible monocations, C-1 protonation is best with the conformation in which OMe group points toward H-3 being 2 kcal/mol lower than the alternative. On this basis the major conformer is assigned to **19aH**$^+$. Raising the temperature to −30 °C gave a conformationally averaged structure (the process was reversible indicative of a conformational equilibrium). The most deshielded protons for **19aH**$^+$/**19bH**$^+$ are the H-4s (δ 9.49/9.35) and the H-11s (δ 8.83/8.73). NOE enhancement is observed between H-4/H-5; H-10/H-11 at the bay regions and between H-1/H-12. The H-5/H-10 protons are significantly shielded relative to the neutral PAH. The C-2 chemical shift (δ 202.9 for **19aH**$^+$ and δ 205.9 for **19bH**$^+$) is indicative of oxonium ion character. Positive charge is extensively localized in the A/B rings at C-2/C-4 followed by C-11/C-12a. Quenching of superacid solution gave back intact **19**.

(**c) 2-Methoxy-11-methylchrysene (20).** Protonation of **20** with FSO_3H/SO_2ClF, in which a bay-region methyl and a methoxy at C-2 compete, resulted in predominant attack at C-1 (*ortho* to OMe) to give **20aH**$^+$ and **20bH**$^+$ as two conformational isomers, in addition to protonation at C-6 (**20cH**$^+$) in 6:3:1 ratio, respectively, at −70 °C (a dark-red homogeneous solution). Carbocations **20aH**$^+$ and **20bH**$^+$ have very similar proton and carbon chemical shifts except in the A ring. Cation **20cH**$^+$ had a conformationally averaged structure even at −70 °C. At −30 °C, the resonances due to **20aH**$^+$/**20bH**$^+$ became coincident, but the signals for H-3, H-4 and C-3, C-4, C-12a were still broad. Irradiation of the methoxy group gave larger NOE enhancement for H-3 than for the CH_2, suggesting that the more predominant conformation was due to **20aH**$^+$. Their relative ratio did not, however, change by warming to −30 °C and by recooling to −70 °C and remained unchanged when the sample was stored for a week at dry ice−acetone temperature. AM1 calculations predicted that **20aH**$^+$/**20bH**$^+$ are indeed the most stable pair of carbocations among all carboxonium pairs that could result by protonation at other sites, and that **20aH**$^+$ is 2 kcal/mol lower in energy than **20bH**$^+$. On the basis of AM1, the minor **20cH**$^+$ is clearly less favored (C-1 > C-3 > C-12 > C-6). The most deshielded proton resonances are the H-4s (δ 9.51 for **20aH**$^+$ and δ 9.37 for **20bH**$^+$), and the most deshielded carbon resonances are the C-2s (δ 200.7 and 204.2). The bay-region H-5/H-10 protons are shielded in the carbocations. The charge is heavily retained in the methoxy-bearing A-ring (C-2/C-4/C-12a) and at C-11, and delocalization into C/D rings is very limited. In **20cH**$^+$, H-5 is most deshielded and H-10 most shielded (δ 9.65 and 8.31). Quenching of the superacid solution led to recovery of skeletally intact **20**.

(d) 2-Methoxy-5-methylchrysene (21). Compound **21** (which was available only in very limited quantity; 4 mg) provided the opportunity to examine the competition between a methyl at the strategic C-5 and a methoxy at C-2 in directing electrophilic attack on chrysene. Low-temperature reaction of **21** with FSO_3H/SO_2ClF gave a dark-red homogeneous solution whose ^1H NMR spectral data are consistent with the formation of two conformationally distinct carboxonium cations **21aH**$^+$/**21bH**$^+$ (in 4:1 ratio) resulting from protonation at C-1. Conformational averaging was observed at −30 °C, but H-3/H-4 still remained broad. AM1 predicted that **21aH**$^+$/**21bH**$^+$ are twisted, and that, in agreement with experiment, they are the most stable pair of carbocations to be formed. Furthermore, AM1 computes **21aH**$^+$ 2 kcal/mol lower than **21bH**$^+$. On this basis the major conformer was assigned to **21aH**$^+$. The most deshielded protons are those of H-4 (δ 10.10 for **21aH**$^+$ and at δ 10.00 for **21bH**$^+$) and H-11 (δ 9.27 for **21aH**$^+$ and δ 9.22 for **21bH**$^+$). NOE enhancements were observed between OMe/H-3; H-1/H-12, and between 5-CH_3/H-4/H-6 and H-10/H-11. Upon quenching, skeletally intact **5** was recovered.

(e) 9-Methyl-4*H*-cyclopenta[*def*]chrysene (22). Low-temperature protonation of **22** in FSO_3H/SO_2ClF gave a 3:1 mixture of **22aH**$^+$and **22bH**$^+$as a dark-red solution. Their ratio remained unchanged at higher temperatures (−70 °C to −50 °C) and upon prolonged storage (1 week at dry ice−acetone temperature). In concert, AM1 calculations predict that among all possible monoarenium cations, **22aH**$^+$ has the lowest energy followed by **22bH**$^+$ which is 0.6 kcal/mol higher. Thus, the site of attack changed from C-5 (in **5** itself) (observed for protonation as well as nitration, bromination)[19d] to predominantly C-11 (in **22**). In **22aH**$^+$ the Me and the methano bridge

Scheme 3

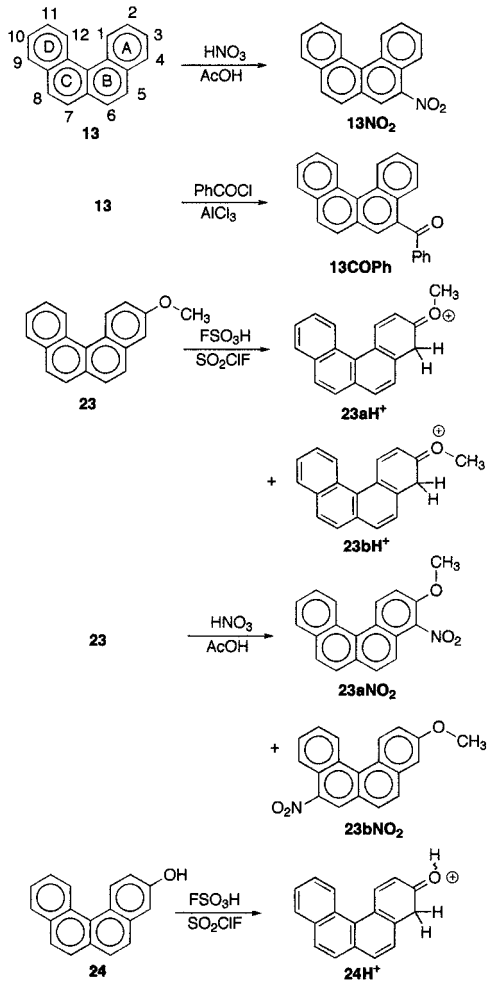

protons move upfield, and in **22bH**$^+$ the Me and H-10 are shielded, whereas other protons are all deshielded with H-10 in **22aH**$^+$ (δ 9.66) and H-11 in **22bH**$^+$ (δ 8.90) being most downfield. For **22aH**$^+$, NOE enhancements were observed between H-1/H-11, H-4/H-3/H-5, H-5/H-6, and 9-Me/H-10. NOE effects for **22bH**$^+$ were detected between H-1/H-11, H-5/H-6, and between 9-Me/H-8/H-10. Charge delocalization in the methanochrysenium ions is clearly more extensive. For **22aH**$^+$ the most deshielded carbons are C-10/C-11a/C-11c (*ortho/para)* and C-5 in addition to C-2/C-8. For **22bH**$^+$ C-4a/C-5a/C-9b/C-11 exhibit the largest charge localization. Quenching of the ion solution cleanly returned the intact PAH.

Electrophilic Chemistry of Benzo[*c*]phenanthrenes (Scheme 3 and Figure S2)

(a) Protonation of BcPh (13). Low-temperature reaction of parent **13** with FSO_3H/SO_2ClF at dry ice−acetone temperature gave a dark-green solution, whose NMR spectra exhibited broad features which are attributed to rapid oligocondensation (or extensive oxidation to the radical cation). Thus parent **13H**$^+$ could not be generated under persistent ion conditions. AM1 minimizations show that the C-5 protonated arenium ion has the lowest energy (followed closely by C-4) and that **13H**$^+$ is slightly twisted.

(b) Nitration and Benzoylation of BcPh (13). In the original report by Newman and Kosak[15a] the nitro, bromo, and acetyl derivatives of **13** were characterized without NMR. More recently, NMR data were given for the acetyl and the bromo derivative, but no specific assignments were made.[15b] Since a persistent carbocation from **13** could not be made, it was appropriate to include electrophilic substitution data with full NMR data for the products. We focused on nitration and benzoylation. Classical nitration of **13** (HNO_3/AcOH) mainly yielded the 5-nitro isomer (**13NO$_2$**) (specific NMR assignments are included in Figure S2). Electrospray mass spectrum (ES-MS) showed *m/z* 274 (M + H)$^+$ and 273 (M$^+$). Friedel−Crafts benzoylation of **13** gave the C-5 benzoylated derivative (**13COPh**) as a main product (Figure S2). Its ES-MS exhibited *m/z* 333 (M + H)$^+$, whose MS/MS gave *m/z* 105 (O=C$^+$Ph) as daughter ion. NOE effects were observed between H-6/H-7 for both **13NO$_2$** and **13COPh**. Nitration at C-5 has a pronounced deshielding effect on H-4/H-6.

3-Methoxybenzo[c]phenanthrene (23). (a) Protonation with FSO_3H/SO_2ClF. Presence of OMe group at C-3 directs the attack to C-4 to generate **23aH**$^+$/**23bH**$^+$ as two conformationally distinct carboxonium ions in 2:1 ratio (between −70 and −50 °C) as a clear red solution with very similar chemical shifts (at −30 °C conformational averaging was observed). AM1 calculations concur by predicting that **23aH**$^+$/**23bH**$^+$ are the most stable carbocations to be formed, and that **23aH**$^+$ is 2 kcal/mol more stable than **23bH**$^+$ and 2 kcal/mol more stable than the next stable cation arising from protonation at C-5. In the ^{1}H NMR, H-1 is most deshielded whereas H-12 is most shielded. NOE effects were observed between H-1/H-12 (across the fjord) and between the C*H*$_2$ and H-5. When the methoxy protons of **23aH**$^+$ were irradiated, NOE enhancement in H-2 was observed, and on this basis the major conformer was assigned to **23aH**$^+$ (this agrees with AM1). The most deshielded carbons for **23aH**$^+$/**23bH**$^+$ are C-1, C-3, and C-4a. The C-3 chemical shift (δ 202.8 for **23aH**$^+$ and δ 206.0 for **23bH**$^+$) is indicative of oxonium ion character. Charge delocalization mapping establishes a clear charge alternation path within the A/B rings (C/D rings not involved). Thus **23H**$^+$ has naphthalenium ion character. Intact **23** was obtained upon quenching of the superacid solution.

(b) Nitration of 23. For comparison, classical nitration (HNO_3/AcOH) of **23** was studied. This gave an isomeric mixture of **23aNO$_2$** and **23bNO$_2$** in 2:1 ratio which was analyzed directly by NMR. For **23aNO$_2$**, NOE enhancements were observed between OMe/H-2 and between H-1/H-12; H-8/H-9. For **23bNO$_2$**, NOE enhancement were detected between H-1/H-12 and H-2/H-4. Methoxy irradiation gave larger enhancement at H-4 than at H-2. The ES-MS spectrum of **23aNO$_2$** and **23bNO$_2$** mixture exhibited *m/z* 304 (M + H), whose MS/MS gave *m/z* 287 (M − O)$^+$ and 258 (M + H − NO$_2$)$^+$ as daughter ions.

3-Hydroxybenzo[c]phenanthrene (24). Similar to **23**, low-temperature protonation of **24** with FSO_3H/SO_2ClF led to attack at C-4 producing **24H**$^+$ (a dark-red solution). This carboxonium cation exists as a conformationally averaged structure even at −65 °C. When CO*H* was irradiated, concurrent NOE enhancement was observed at H-2/H-4; however, the enhancement for H-2 was larger than for H-4. AM1 agrees, predicting the conformer with OH pointing toward H-2 to be 2 kcal/mol lower in energy. It also computed **24H**$^+$ as the most favored carbocation having a twisted minimized structure. Additional NOE effects were detected between H-1/H-12 (across the fjord) and between H-4/H-5, H-8/H-9.

Scheme 4

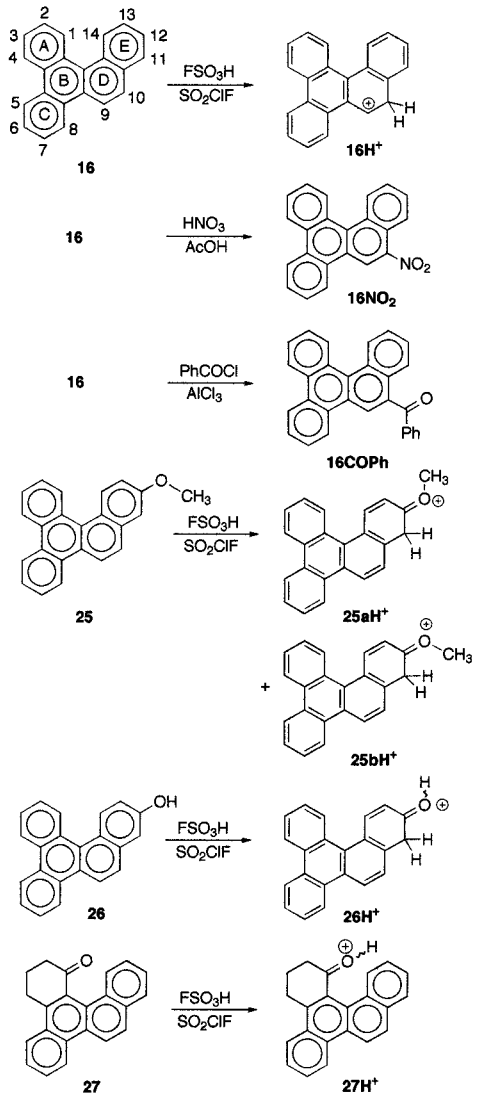

The most deshielded protons (at −50 °C) are the O*H* (*δ* 11.05), H-1 (*δ* 9.76), and H-6 (*δ* 8.40); whereas H-12 is strongly shielded. The most deshielded carbons are C-1 (*δ* 173.0), C-3 (*δ* 203.7), C-4a (*δ* 144.6), and C-6 (*δ* 140.2). Positive charge is localized in the A/B rings. Quenching of the ion solution gave back the intact **24**.

Electrophilic Chemistry of Benzo[g]chrysenes (Scheme 4 and Figure S2)

Parent Benzo[*g*]chrysene BgCh (16). (a) Protonation. Low-temperature reaction of **16** with FSO_3H/SO_2ClF gave the arenium ion **16H**$^+$ (regiospecific protonation at C-10) as a dark-green solution. In line with experiment, AM1 predicts that C-10 protonation is most favored. Initially, the ^{1}H NMR spectra showed some line-broadening (concomitant presence of the radical cation!), but this soon vanished during the measurements at −70 °C. A notable feature is the nonequivalence of the CH_2 protons which appeared as two slightly broad doublets (*δ* 4.28 and 4.03). The observed geminal coupling of 31 Hz corresponds to a HCH angle of ca. 101°. The diastereotopic nature of the C-10 methylene protons is a consequence of the pseudo-helical structure of **16H**$^+$ (AM1 supports a twisted minimum). This phenomenon was previously observed in hexahelicenium cations.[24] Another notable feature is paratropicity of this cation, whereby most of the protons are *shielded* as compared to the neutral BgCh (H-1/H-14 in the fjord region are most shielded). The center of gravity in the ^{1}H NMR in the aromatic region was 7.96 ppm at −70 °C and that of neutral precursor 8.16 ppm. NOE enhancements are observed between H-10/H-11, H-8/H-9, H-1/H-14. The most deshielded carbons are C-3, C-4a, C-9, C-10a, and C-14b. Charge delocalization mode is quite interesting; it involves the D/E and the A rings and could best be visualized as a phenylnaphthalenium ion. Intact **16** was recovered upon quenching with cold methanol.

(b) Nitration and Benzoylation. In agreement with protonation, classical nitration of **16** (HNO_3/AcOH) yielded the 10-nitro derivative (**16NO$_2$**), and the Friedel−Crafts benzoylation gave the C-10 benzoylated derivative (**16COPh**). For the latter, NOE enhancements were observed between H-8/H-9 and between H-9 and Ph (*ortho*-H), showing that the benzoyl phenyl is *down* (close to K-region). Nitro substitution induces a larger *ortho* deshielding effect in **16NO$_2$** (H-9 at *δ* 9.36) as compared to **13NO$_2$** (H-5 at *δ* 8.57). The electrospray mass spectrum of **16NO$_2$** exhibited *m*/*z* 324 $(M + H)^+$, whose MS/MS gave *m*/*z* 307 $(M - O)^+$ and 278 $(M + H - NO_2)^+$ as daughter ions. The ES-MS of **16COPh** showed *m*/*z* 383 $(M + H)^+$, whose MS/MS gave *m*/*z* 305 $(M - Ph)^+$.

12-Methoxybenzo[g]chrysene (25). Low-temperature reaction of **25** with FSO_3H/SO_2ClF gave a dark-red solution with concomitant formation of some red precipitation (at −70 °C) which dissolved upon storage of the sample at −70 °C. The NMR data are consistent with protonation at C-11 leading to two conformationally distinct carboxonium ions **25aH**$^+$/**25bH**$^+$ (2:1 ratio). Whereas their O*CH*$_3$ groups are coinciding, their *CH*$_2$'s are different. Conformational averaging occurred on raising temperature to −30 °C. AM1 calculations predict that **25aH**$^+$/**25bH**$^+$ are indeed the most stable pair of carboxonium ions and that **25aH**$^+$ is 2 kcal/mol more stable than **25bH**$^+$. Their overall chemical shift patterns are very similar. As with **16H**$^+$, there is a dramatic paratropic shift of the ring protons. The center of gravity for the aromatic protons are *δ* 7.80 (**25aH**$^+$) and *δ* 7.79 (**25bH**$^+$) at −70 °C, whereas that of the neutral precursor is *δ* 8.11. The most deshielded carbons are C-12/C-14/C-10a (*ortho*/*para*) and C-9. NOE enhancements were observed for the bay-region and fjord region protons (H-4/H-5; H-8/H-9; H-1/H-14) and between OMe/H-13 at −30 °C. Positive charge is highly localized in the D/E rings. Intact **25** was recovered upon quenching.

12-Hydroxybenzo[*g*]chrysene (26). Analogous to **25**, low-temperature protonation of **26** (FSO_3H/SO_2ClF) leads to attack at C-11 (a clear-red solution). Initial proton spectra were somewhat broad but sharpened on raising the temperature to −50 °C. As with of **24**, only a conformationally averaged carboxonium ion is formed (spectra remained unchanged, although at −30 °C the H-9/H-10 doublets broadened). AM1 predicts that the minimized structure **26H**$^+$ is twisted at the fjord region, and that it is the lowest energy carbocation. NOED spectra showed NOE effect between H-11/H-10, H-9/H-8, and H-1/H-14. As with other BgCh cations a dramatic paratropic shift of the proton resonances is observed for **26H**$^+$, with the center of gravity of the aromatic protons at *δ* 7.73 as compared to **26** at *δ* 8.11. A clear charge

(24) Laali, K. K.; Houser, J. J. *J. Chem. Soc. Perkin Trans. 2* **1994**, 1303.

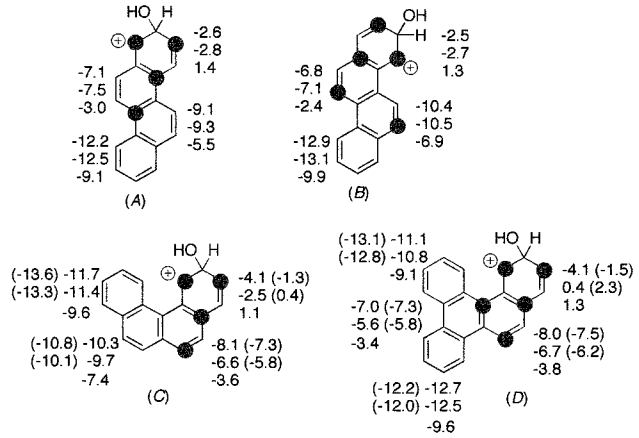

Figure 1. Ab initio/GIAO-derived charge delocalization mode and calculated NICS values (at 1.0 and 0.5 Å above each ring centroid and at each ring centroid, respectively) for hydroxy-substituted carbocations (values outside parentheses are measured with OH group on the same side and inside parentheses with OH group on the opposite side. [For benzene: NICS (1.0) = −12.7; NICS (0.5) = −12.5; NICS (0.0) = −9.9.]

alternation path can be defined within a naphthalenium ion in the D/E ring. The intact substrate was recovered upon quenching. In an attempt to generate a carboxonium−arenium dication by further ring protonation, **26** was reacted with FSO_3H-SbF_5 (4:1)/SO_2ClF; a dark-brown precipitate was formed instead.

1,2,3,4-Tetrahydrobenzo[*g*]chrysen-1-one (27). Compound **27** is a synthetic precursor to the fjord-region tetrahydro-epoxide which is a better DNA-alkylating agent than **18a**/**18b**.[23] Since **17a**/**17b** are the ultimate carcinogens but not **18a**/**18b**, it was of interest to compare charge delocalization and relative stabilities in the two types of fjord-region carbocations. Protonation of **27** was included in this study. Its low-temperature reaction with FSO_3H/SO_2ClF gave the carboxonium cation **27H**$^+$ as a red solution which exhibited broad NMR features at −70 °C due to the formation of a mixture of conformationally distinct cations, which averaged upon raising the temperature, giving rise to sharp resonances at to −20 °C (this phenomenon was reversible). At this temperature the COH^+ signal coalesced with the acid peak (δ 10.86). AM1 minimizations computed the "*in*-form" 6 kcal mol^{-1} lower in energy than the "*out*-form". This is presumably a result of significant distortion of the E-ring, allowing an easy fit for the O*H* into the pitch of the cation (AM1-minimized structures of **27H**$^+$ and **27** are included in Supporting Information). In the resulting twisted carboxonium ion, C-1 (δ 206.5), C-14c, and C-10 are most positive, but there is no clear charge alternation path. In fact, adjacent positive charges are observed for several carbons within the chrysene moiety, while C-4a/C-8a are noticeably shielded. These features must stem from its twisted structure!

Theoretical Studies (Figure 1). The hydroxy-carbenium ions A−D derived from the corresponding epoxides of BcPh, BgCh, and Ch were examined by the ab initio/GIAO method.[25] Based on the calculated ^{13}C NMR chemical shifts, the charge delocalization pattern sketched in Figure 1 may be derived. Computed NICS values[26] complement these patterns, illustrating that the remote rings which are significantly less involved in charge delocalization remain most aromatic.[27]

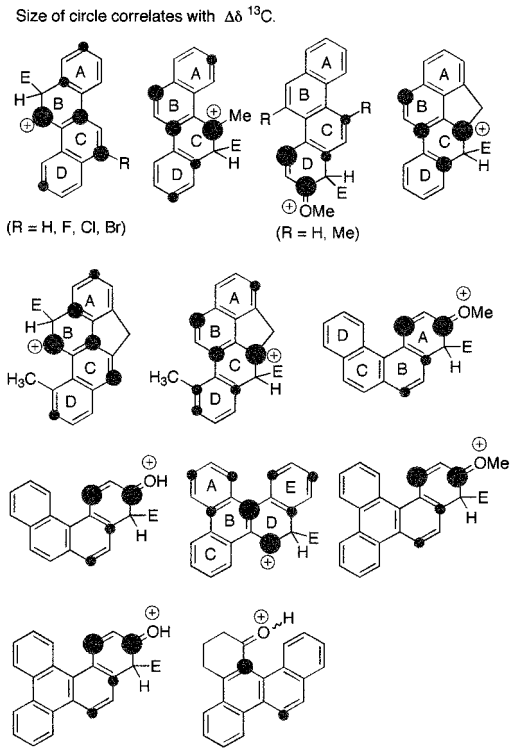

Figure 2. ^{13}C NMR-derived charge delocalization mode in the carbocations and carboxonium ions.

Comparative Discussion of Substituent Effects vs Charge Delocalization Mode (Figures 1 and 2). In parent Ch and its 6-halo-substituted derivatives C-12 is the protonation site and positive charge is mostly localized in the B/C rings.[19d] A C-5 methyl substituent directs the attack predominantly to C-6, this generates a complementary charge alternation path, i.e., B/C rings but opposite carbons! A methoxy at C-2 directs the attack to C-1 forming a carboxonium ion whose charge delocalization pattern is confined to the D/C rings. The site of attack remains unchanged (C-1) when a methyl group is introduced at either bay region (C-11 or C-5), and positive charge is localized in the C/D rings. In 4*H*-cyclopenta[*def*]chrysene attack is directed to C-5 (*peri* to methano bridge) with charge residing in the C/B rings. Introduction of methyl into C-9 led to attack at C-12 and C-5. Charge delocalization in these carbocations is more extensive. On the basis of ab initio/GIAO calculations (Figure 1), the hydroxy-chrysenium ion (**B**) resulting from 3,4-epoxide ring opening is more delocalized (A/B rings plus one conjugated carbon) than **A** formed via 1,2-epoxide opening (the A-ring plus one conjugated carbon). This is in line with DNA binding studies which identifies C-4 as the binding site to form dG and dA adducts.[9b]

For parent BcPh electrophilic attack is directed to C-5 (nitration and benzoylation). In the 3-methoxy and 3-hy-

(25) Wollinski, K.; Hinto, J. F.; Pulay, P. *J. Am. Chem. Soc.* **1990**, *112*, 8251; Ditchfield, *Mol. Phys.* **1974**, *27*, 789.

(26) Schleyer, P.v. R.; Maerker, C.; Dransfeld, A.; Jiao, H.; Hommes, N. J. R. v. E. *J. Am. Chem. Soc.* **1996**, *118*, 6317.

(27) NICS values were determined at 1.0 and 0.5 Å above each ring centroid and at each ring centroid. The computed values (sketched in Figure 1) infer sequential decrease in aromaticity, but the overall trend remains the same (we thank one of the reviewers for suggesting that we check into possible effects of distance on NICS values in these delocalized PAH carbocations).

droxy derivatives, C-4 is the site of attack, and positive charge is heavily retained in the A-ring. Although the charge delocalization mode in protonated BcPh (not observed) could not be determined, theory predicts that positive charge in the hydroxy-arenium ion (**C**) formed by opening of its fjord-region epoxide resides heavily in the A/B rings (Figure 1). This is a logical intermediate for covalent attachment to the exocyclic amino group of dG and dA.[7] The electrophilic chemistry of BgCh overwhelmingly points to C-10 as the site of attack. Charge delocalization mapping generates a delocalization path that involves the D/E rings as well as the A ring, i.e., phenylnaphthalenium ion character. Introduction of OMe or OH into C-12 directs the incoming electrophile to C-11. In these cations there is a regular charge alternation path within the D/E rings (naphthalenium ion). This pattern is quite different from that in **27H**$^+$. In good correspondence with our experimental models, the theoretically predicted pattern for the hydroxy-arenium ion (**D**) formed via BgCh 13,14-epoxide ring opening is one where the positive charge resides in the D/E rings (Figure 1). Carbocation (**D**) is, therefore, a logical intermediate to link to the N-6-amino group of dA or dG.[28]

Among the BgCh carbocations the methoxy- and hydroxy-substituted analogues with more localized charge are more paratropic than the parent **16H**$^+$ whose charge is more delocalized. The observed paratropicity must stem from a combination of charge localization and the pseudohelical structure which is most significant for BgCh (chrysenium, benzo[*c*]phenanthrenium, and benzo[*g*]chrysenium cations are all 4nπ systems).

Experimental Section

The precursors used in this study were synthesized by Kumar employing a Suzuki coupling reaction as a key step (synthetic details are already reported).[21] Compound **22** was a gift from Prof. R. G. Harvey (Ben May Institute, University of Chicago). Compound **27** (ref 23) was a gift from Prof. Lehr (University of Oklahoma).

FSO_3H (Allied and Aldrich) and SbF_5 (Aldrich and Fluorochem) were freshly distilled in an all-glass distillation unit under a dry nitrogen atmosphere. SO_2ClF was synthesized from SO_2Cl_2, ammonium fluoride, and trifluoroacetic acid according to a modified procedure of Prakash et al.[29] Several distillations provided pure SO_2ClF. Other commercially available reagents were used as received.

NMR spectra were recorded on a 500 MHz spectrometer. Those of neutral PAHs were recorded in $CDCl_3$ at room temperature. Carbocations were studied between −70 °C and −30 °C. NMR analyses included ^{1}H, ^{13}C, H/H COSY, C/H HETCOR (or HMQC), COLOC (or HMBC), and NOED experiments.

AM1 Calculations. These were carried out using standard methods as implemented in the Hyperchem package version 5.11 (Hypercube Inc, 1999) or Insight II Release 97.0 (MSI, 1999).

Model ab initio calculations were performed with the Gaussian 98 software.[30] NMR chemical shifts were calculated by GIAO/B3LYP/6-31G(d,p). NICS values were obtained with GIAO/3-21G at the ring centroid (NICS (0.0)) and at points 0.5 and 1.0 Å above and below the ring centroid (NICS (0.5) and NICS (1.0), respectively).

Mass Spectra. These were obtained using electrospray MS (an ion-trap instrument with MS/MS capability). Acetonitrile−water (1:1) was used as solvent to which 0.01% NH_4NO_3 was added to protonate the PAH.

General Procedure for Stable Ion Generation. SO_2ClF (ca 0.4 mL) was distilled into a 5 mm NMR tube containing the PAH (5−20 mg) cooled to dry ice−acetone temperature. To the resulting suspension was carefully added cold FSO_3H (2 drops) or cold FSO_3H-SbF_5 (4:1) (2 drops), and the mixture was mixed (vortex) until homogeneous. Then two drops of cold CD_2Cl_2 were added on the top of the solution, and the mixture was thoroughly mixed (vortex).

Quenching Experiments with Water. The superacid solution was carefully poured into ice−$NaHCO_3$, and the mixture was extracted with CH_2Cl_2. The organic extract was washed (10% NaCl) and dried ($MgSO_4$). The solvent was removed under reduced pressure, and the residue was analyzed by NMR.

Quenching Experiment for 6 with Methanol. The superacid solution was carefully poured into cold methanol. Most of the solvent was evaporated, and the residue was dissolved in CH_2Cl_2. The solution was washed (sat. NaCl) and dried ($MgSO_4$), and the solvent was removed under reduced pressure and examined by NMR.

Nitration of Benzo[c]phenanthrene (13). To a solution of **13** (10 mg, 0.044 mmol) in CH_2Cl_2 (0.1 mL) were added AcOH (0.1 mL) and 50% HNO_3 (0.1 mL), and the mixture was stirred overnight. The reaction mixture was poured into water. The organic layer was extracted with CH_2Cl_2, washed (10% NaOH), and dried ($MgSO_4$). After removal of the solvent, the residue was passed through a short column of SiO_2 (using CH_2Cl_2) from which **13NO$_2$** (10 mg) was obtained as a yellow oil. Complete NMR data (Figure S2; Supporting Information); mass spectral data (see Discussion).

Benzoylation of Benzo[*c*]phenanthrene (13). To a solution of **13** (10 mg, 0.044 mmol) in CH_2Cl_2 (1 mL) was added a mixture of PhCOCl (10 mg, 0.071 mmol) and $AlCl_3$ (50 mg, 0.38 mmol). The reaction mixture was stirred for 1 h, and water was added. The resulting solution was extracted with CH_2Cl_2; the organic layer was washed (10% NaOH) and dried ($MgSO_4$). Removal of solvent gave pale yellow crystals. Column chromatography [SiO_2, CH_2Cl_2−pentane (1:1)] gave **13COPh** (5 mg, 34%) as a yellow oil. IR (KBr) 1654 cm^{-1}. Complete NMR data (Figure S2; Supporting Information); mass spectral dtat (see Discussion).

Nitration of 3-Methoxybenzo[*c*]phenanthrene (23). To a solution of **23** (5 mg, 0.019 mmol) in AcOH−CH_2Cl_2 (1:1) (0.2 mL) was added 50% HNO_3 (0.1 mL), and the mixture was stirred overnight. The solution was poured into water and extracted (CH_2Cl_2), and the organic layer was washed (10% NaOH) and dried ($MgSO_4$). Evaporation of the solvent gave **23aNO$_2$** and **23bNO$_2$** as an isomeric mixture (2:1); yellow oil (5 mg). Complete NMR data (Figure S2; Supporting Information); ES-MS (see Discussion).

Nitration of Benzo[*g*]chrysene (16). A similar procedure as for **13** was utilized. Following the reaction and workup, removal of the solvent gave **16NO$_2$** (5 mg, 86%) as yellow crystals which were analyzed by NMR (Figure S2; Supporting Information), ES-MS (see Discussion), IR ($CHCl_3$): 1520, 1344 cm^{-1}; mp 175−178 °C.

Benzoylation of Benzo[*g*]chrysene (16). A similar procedure as for benzoylation of **13** was utilized. Following the reaction and workup, the solvent was removed to give pale-

(28) Kiselyov, A. S.; Steinbrecher, T.; Harvey, R. G. *J. Org. Chem.* **1995**, *60*, 6129.

(29) Reddy, V. P.; Bellow, D. R.; Prakash, G. K. S. *J Fluorine Chem.* **1992**, *56*, 195.

(30) Gaussian 98 (Revision A.7), Frisch, M. J.; Trucks, G. W.; Schlegel, H. B.; Scuseria, G. E.; Robb, M. A.; Cheeseman, J. R.; Zakrzewski, V. G.; Montgomery, J. A.; Stratmann, R. E.; Burant, J. C.; Dapprich, S.; Millam, J. M.; Daniels, A. D.; Kudin, K. N.; Strain, M. C.; Farkas, O.; Tomasi, J.; Barone, V.; Cossi, M.; Cammi, R.; Mennucci, B.; Pomelli, C.; Adamo, C.; Clifford, S.; Ochterski, J.; Petersson, G. A.; Ayala, P. Y.; Cui, Q.; Morokuma, K.; Malick, D. K.; Rabuck, A. D.; Raghavachari, K.; Foresman, J. B.; Cioslowski, J.; Ortiz, J. V.; Stefanov, B. B.; Liu, G.; Liashenko, A.; Piskorz, P.; Komaromi, I.; Gomperts, R.; Martin, R. L.; Fox, D. J.; Keith, T.; Al-Laham, M. A.; Peng, C. Y.; Nanayakkara, A.; Gonzalez, C.; Challacombe, M.; Gill, P. M. W.; Johnson, B. G.; Chen, W.; Wong, M. W.; Andres, J. L.; Head-Gordon, M.; Replogle, E. S.; Pople, J. A. Gaussian, Inc., Pittsburgh, PA, 1998.

yellow solid. Column chromatography [SiO_2, CH_2Cl_2−pentane (1:1)] gave **16COPh** (2 mg, 30%) as pale yellow crystals: IR ($CHCl_3$) 1656 cm^{-1}; NMR analysis (Figure S2; Supporting Information) and ES-MS (see Discussion).

Acknowledgment. Support of our work under mechanistic carcinogenesis by the NCI of NIH (R15 CA 78235-01A1) is gratefully acknowledged. We thank Dr. M. Gangoda for assistance with high field NMR and ES-MS. S.E.G. thanks LCCA-USP for generous allocation of computational resources.

Supporting Information Available: Figure S1 and Figure S2. Selected NMR spectra for the protonation of **3**, **16**, **19**, **20**, **21**, **24**, **25**, and **26** and the AM1 minimized structures for **27** and **27H**$^+$. This material is available free of charge via the Internet at http://pubs.acs.org.

JO001268B